Analysis and initial design of bidirectional acoustic tag modulation schemes and communication protocol

Daniel Corregidor
Instrumentation and Applied Acoustics Research Group (I2A2), Universidad Politécnica de Madrid. Madrid, Spain
daniel.corregidor@i2a2.upm.es

Ivan Masmitja
SARTI Research Group, Electronics Department
Universitat Politècnica de Catalunya
Barcelona, Spain
ivan.masmitja@upc.edu

Juan Manuel López
Instrumentation and Applied Acoustics Research Group (I2A2), Universidad Politécnica de Madrid. Madrid, Spain
juanmanuel.lopez@upm.es

Spartacus Gomariz
SARTI Research Group, Electronics Department
Universitat Politècnica de Catalunya
Barcelona, Spain
spartacus.gomariz@upc.edu

Joan Navarro
Institut de Ciències del Mar
Barcelona, Spain
joan@icm.csic.es

Guillermo de Arcas
Instrumentation and Applied Acoustics Research Group (I2A2), Universidad Politécnica de Madrid. Madrid, Spain
g.dearcas@upm.es

Abstract*—Acoustic underwater tags are key devices to study marine animals and obtain information regarding their behaviour. This information is essential to increase our knowledge of oceanic species and implement efficient conservation policies. At present, all the acoustic tags have a unidirectional communication protocol, which introduces important limitations for their localization such as range measurement, and in situ reconfiguration. To solve these issues and improve the current state-of-the-art of acoustic tags, a new bidirectional tag device has been developed. This new tag will allow new studies and will open a wide tracking capability by using autonomous underwater vehicles and range-based algorithms. The main characteristics of the tag communications scheme such as the chosen modulation, its implementation and the communication protocol are presented on this paper. Also, the simulation software and the conclusions that lead to the initial prototype design are presented.

Keywords—Bidirectional, acoustics, tags, underwater simulations, communications, digital modulations, marine species

I. INTRODUCTION

Acoustic underwater tags are key devices to study marine animal behaviours. An important field of marine animals' behaviour study is their movements because if we are able to increase our knowledge of their spatial behaviour and comprehend their patterns, our capabilities to implement new conservation policies also increases [1]. Several devices are available on the market from manufacturers like Vemco or Sonotronics which implements different digital acoustic based communication protocols to send data from the tag to the receiver unit. A crucial point of these devices is the chosen modulation scheme and its robustness regarding the effects of the underwater channel which is very aggressive in terms of signal degradation[2].

Several advances have been made on the underwater acoustic communications field during the past decades. These have been motivated by the need of developing sophisticated systems to support ocean exploration, ocean studies or marine animals' studies [3]. Some of these developments include bandwidth optimization, adaptation to the effects introduced by the underwater channel or Software Defined Radio (SDR) applied to underwater acoustic modems [4][5][6][7]. Additionally, advances have been made in the field of signal processing to increase the bit-rate, channel estimation with equalization purposes, time synchronization and the use of new modulations schemes such as OFDM [8][9][10][11][12][13]. Moreover, several studies model the underwater channel and its effects on underwater wireless communications leading to different approaches such as raytracing [14][15] or statistical characterization [16]. Simulation tools are essential to evaluate new protocols or algorithms before testing them in real field environments, minimizing development time and cost. This simulation-based approach has been used on the initial design stage of the new miniaturized acoustic tag and its communication protocol which is presented in this paper.

Following the objective of improving tracking of marine species, a miniaturized bidirectional acoustic tag (B-tag) has been designed. This new device adds new capabilities and break the current limitation of the existing market tags, adding new features such as: tag configuration after deployment, capability to compute time to flight (TOF) between tag and receiver allowing the estimation of distances. This tag shows three

This work received financial support from the Spanish *Ministerio de Economía y Competitividad* (contract TEC2017-87861-R project RESBIO, RTI2018-095112-B-I00 project SASES, and CTM2017-82991-C2-1-R project RESNEP), from the *Generalitat de Catalunya* "*Sistemas de Adquisición Remota de datos y Tratamiento de la Información en el Medio Marino* (SARTI-MAR)" 2017 SGR 371. J. Navarro was funded by the Spanish National Program Ramón y Cajal (RYC-2015-17809). This project has also received funding from the European Union's Horizon 2020 research and innovation programme under the Marie Skłodowska-Curie - Individual Fellowship grant agreement AIforUTracking No 893089.

transmission predefined working modes: polling-based, silent mode and Mixed mode[x]. These capabilities let the tag can be used to create an underwater wireless sensor network (UWSN).

The proposed bidirectional tag implements a software layer that performs all the modulation and demodulation tasks through a low power consumption microcontroller. The modulation schemes and algorithms have been tested through simulations using Bellhop ray-tracing module of the Acoustic-Toolbox software [15] and its python wrapper Arlpy to generate a simulation of the underwater acoustic channel. The design simulations and the microcontroller modulations software layer are presented on this paper.

II. BRIEF HARDWARE DESCRIPTION OF BIDIRECTIONAL TAG

The bidirectional tag has been designed as a miniaturized acoustic bidirectional device for long term experiments with small species. Thus, the main design objectives for this tag are low power consumption and small size but preserving its computational capabilities as high as possible. Miniaturized electronics have been used to meet the tag size requirements. All the electronics have been mounted on a 33.5 x 10 x 0.4 mm PCB board as shows Fig. 1. All elements have been chosen to maximize this requirement and a very strict software and hardware power management system have been implemented. The main unit of the tag is an ARM cortex-M4 based microcontroller (STM32L432KCU6, ST Microelectronics, USA). This unit have been chosen because of its computational capabilities due to a floating-point unit (FPU), a digital signal processor (DSP) instructions set, and its low power consumption. In addition, the microcontroller implements an analog to digital converter (ADC) and digital to analog converter (DAC) capabilities in order to transmit and receive modulated data. Also, the microcontroller includes sleep mode capabilities, so it is able to reduce the power consumption. In this way the microcontroller is in sleep mode until it is waked-up by a master unit through a wake-up signal. Among with the main processing unit several sensors can be added, for example, the first version of the B-tag includes an eCompass module (LSM303AGRTR, ST Microelectronics, USA) with an ultra-low power 3D accelerometer and a magnetometer.

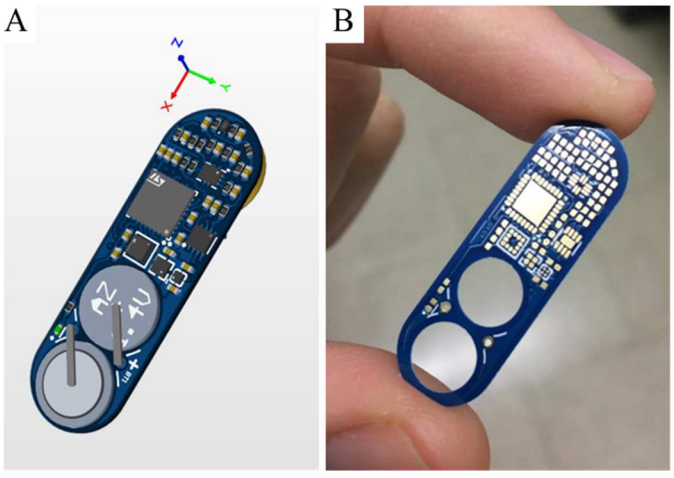

Fig. 1 (A) Bidirectional tag 3D model. (B) Manufactured PCB (33.5 x 10 x 0.4 mm)

The main tasks of the microcontroller are:

- Managing communications according to the chosen protocol, i.e. demodulate and analyse received data and generate response modulated frame according to the received instructions
- Acquiring data from external sensors
- Managing sleep-mode and operation mode switching through the wake-up chirp signal
- Computing range measurement between two devices

In addition to the microcontroller, the tag includes the following elements:

- Miniaturized (10x10 mm) piezoelectric transducer for acoustic communications
- Signal conditioning system composed by a preamplifier, an attenuator network and a band pass filter (BPF)
- Piezoelectric driver to boost the transmission signal

III. MODULATIONS AND SOFTWARE IMPLEMENTATION

After the main hardware components have been presented, the main characteristics of the chosen modulation scheme and its software and simulation implementation are detailed in this section, such as the basis of the communication protocol.

A. Modulation

Different modulations have been tested through simulation using the *arlpy* python package, which is a wrapper for the *Bellhop* beam/ray trace code of *Acoustic Toolbox* package. Finally, a frequency-shift keying (FSK) modulation has been chosen, due to its robustness under reduced signal to noise ratio (SNR) and simplicity to be implemented in small microcontrollers such as the STM32L432KCU6. Its simplicity allows to reduce microcontroller resources consumption (i.e. memory and power consumption) as much as possible which is one of the main design objectives. Two symbols have been chosen, one for logic ones and the other for logic zeros. The symbols frequencies are 47,5 kHz and 52,5 kHz ($\Delta f = \pm 2{,}5$ kHz) so the modulation bandwidth is 5 kHz. The modulation carrier frequency is 50 kHz, although it can be switched to a different value depending on the transducer performance and its frequency response to optimize the overall performance. Moreover, the microcontroller must manage modulation and demodulation operations in order to be able to perform bi-directional communications so both a digital modulation and a digital demodulation module have been implemented. All the input-output processes run through a ADC working at 125kHz@12bits and an DAC working at 1MHz@12bits.

The FSK data encoding is performed as shows Fig. 2 A). The incoming bit stream is encoded according to FSK modulation:

- Logic ones: Symbol frequency 1 (47,5 kHz)
- Logic zeros: Symbol frequency 2 (52,5 kHz)

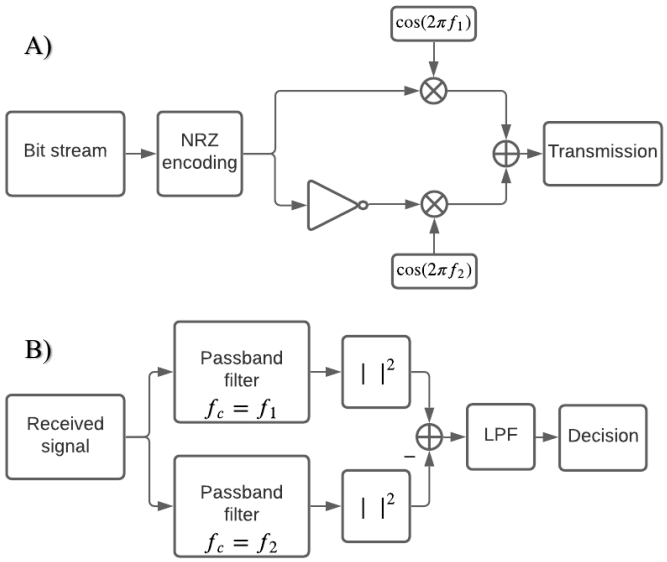

Fig. 2 Modulation (A) and demodulation (B) block diagrams. The bit stream is NRZ encoded, then, each symbol is generated according to its associated frequency (f1 and f2) and both signals are added and transmitted. Demodulation is performed in a non-coherent way through pass-band filtering and decision stage based on a fixed threshold.

Symbol duration is chosen according to target bitrate and microcontroller/modulation limitations. Also, traditional approaches for inter-symbol interference (ISI) avoidance expects that the symbol duration of the transmitted signal to be larger than the channel delay spread [18] so the larger the symbol the better performance against ISI but less bit-rate. In consequence, symbol duration must be chosen in terms of expected modulation strength against underwater multipath effect, evaluating the trade-off between bitrate and ISI. Nevertheless, the tag objective is not to perform continuous communications neither transmits very large data sets, so we can increase symbol length, and in consequence, reduce bitrate to improve signal strength. In this way, TABLE *I* shows four possible bit rates depending on the selected symbol length and the DAC sampling frequency.

TABLE I RELATION BETWEEN SYMBOL LENGTH, NUMBER OF SAMPLES AND TARGET BITRATE

Symbol length (ms)	12,5	6,25	3,125	0.79
Samples/symbol	12500	6250	3125	798
bps	80	160	320	1250

The resulting FSK frame is delivered to the DAC through a DMA ping-pong buffer continuously filled with signal samples.

On the receiver module, all the data is processed in real time. Therefore, once the tag has been waked-up and it is synchronized, the incoming signal will be processed as it comes. The processing chain is composed of a ping-pong DMA based buffer that delivers continuous frames from ADC to the non-coherent demodulator. Next, each delivered frame is filtered by two 17 coefficients FIR pass-band filters tunned to symbols frequency. Then, in order to obtain the base-band signal, the energy of each filter's output is computed and both signals are subtracted followed by a 24 coefficients FIR low pass filtering operation tuned to a frequency equals to the symbol rate. The resulting frame is sampled at symbol period and compared against a fixed threshold to detect logic 1 or logic 0.

In order to evaluate time consumption of the different modulation and demodulation modules, execution time of one symbol generation has been measured for different combinations of symbol length and microcontroller clock frequencies. Fig. 3 shows results of modulation module for clock frequencies between 10 and 80 MHz and for symbol lengths of 3,192 ms, 1,596 ms, 0,798 ms and 0,399 ms. As we can see, the microcontroller is able to generate a symbol in less time that is needed to transmit it, so the execution time of the modulation module for this symbol length range, is not a limitation in terms of computational capabilities. In this way, while the current symbol is been transmitted, next symbol can be generated in less time than the transmission time.

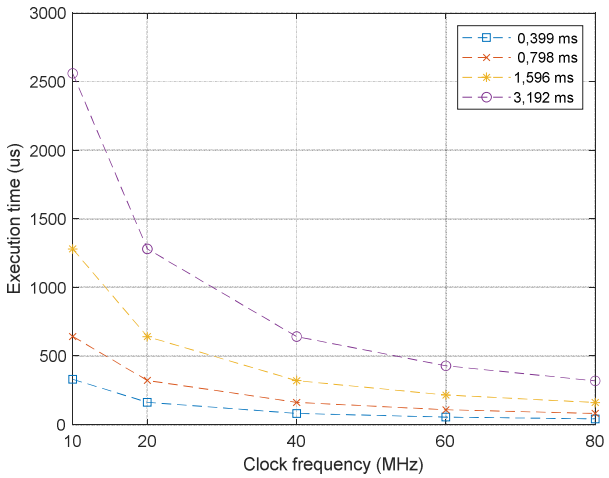

Fig. 3 Measured execution time for modulation module for different combinations of microcontroller clock frequencies and FSK symbol length

Also, demodulation time for 1 FSK symbol (0.798 ms symbol length) has been measured for a 60 MHz clock frequency, which is an optimized value for the ADC sampling frequency (125 kHz). A complete symbol is captured in 800 µs and the measured processing time is 360 µs. Therefore, this processing time allows the system to capture and process a complete symbol in real time.

B. Communication protocol

The communication protocol is based on a master-slave multidrop protocol [19] where the master unit is another tag or an acoustic modem. Each tag has a unique identifier (id) so, when the communication is initiated by the master unit, the tag will only respond if its own id is addressed by the master unit.

Under this scheme, the communication frame is composed by a 5 ms initial chirp signal, centred on 50 kHz, for microcontroller wake-up purpose. The initial chirp is followed by a blank space and another chirp signal to synchronize the tag and generate an accurate reception timestamp. The second chirp

signal is followed by another blank space and the FSK frame. The FSK frame is composed by an initial start byte corresponding to 0xAA hexadecimal value and an 8 bits unique tag id. This unique id allows the deployment of multiple tags on the same scenario so the received information can be associated to specific tags. The payload data that follows tag id is a configurable length frame. The payload data may contain information regarding user commands with configuration instructions or data collected by the tag sensors which have been required by the master unit. Finally, a checksum is added to the end of the frame.

Three different predefined functionalities have been implemented on the tag which allow different working modes. The first functionality is the pooling-based mode (Fig. 4A) where the master unit initiates the communication. The tag receives a query by the master unit and a response is generated with the requested information which is transmitted during a time slot. This query can be sent to a single tag or to multiple tags. The second functionality is the silent mode transmission (Fig. 4B) where the tag continuously transmits packages separated with a fixed period of time. In addition, the reception module is switched off, and therefore the tag works on a low power consumption mode which allows an extended tag's life expectancy. Finally, the third functionality is the mixed mode that combines the first two functionalities (Fig. 4 C). The B-tag is in sleep mode most of the time but when a message is sent the reception module stills switched on during a time window where the master unit is able to interrogate the tag.

C. *Modulation simulations*

Several scenarios have been simulated to evaluate the modulation performance through the underwater acoustic channel. The software architecture used for simulations is shown on Fig. 5. It is formed by a configuration block that feeds different parameters to the Bellhop and the modulation blocks such as symbols frequencies and length, scenario bottom depth and range, sound speed profile and transmitter's and receiver's depth. The modulation block composes the FSK frame, including modulated data and other frame elements such as synchronization chirps. Then, the FSK frame is processed through the underwater channel which includes the impulse response generated by Bellhop and gaussian noise. The resulting signal is received by the demodulator module that performs the chirp-based synchronization and demodulation of FSK frame as shows Fig. 2 B). Finally bit error rate is computed to evaluate modulation performance over the simulated scenario.

Fig. 6 and Fig. 7 show two examples of a received signal and a demodulated baseband signal, respectively. The simulation scenario is 350 meters depth, where the transmitter is fixed on the bottom and the receiver is at 200 meters depth and its separation is 30 meters. The main parameters of the signal are the same described on section III.A. Symbol length is 3.192 ms and the estimated bitrate is 300 bps for Fig. 6 and 12.5 ms and 80 bps for Fig. 7. The received signal shown on Fig. 6, is composed by the synchronization chirp signal, a blank space and a 32-bit FSK frame. Fig. 7 shows the demodulated baseband signal. As it has been said, before demodulation, the incoming signal is synchronized through a correlation process with the chirp signal, so the resulting demodulated signal can be sampled at symbol time accurately.

Next, with the objective of defining the best operating areas for the tags, a 500 meters depth and 200 meters range simulation scenario has been defined with Bellhop. This simulation scenario provides a tool to simulate the modulation performance against the multipath effect of the underwater acoustic channel.

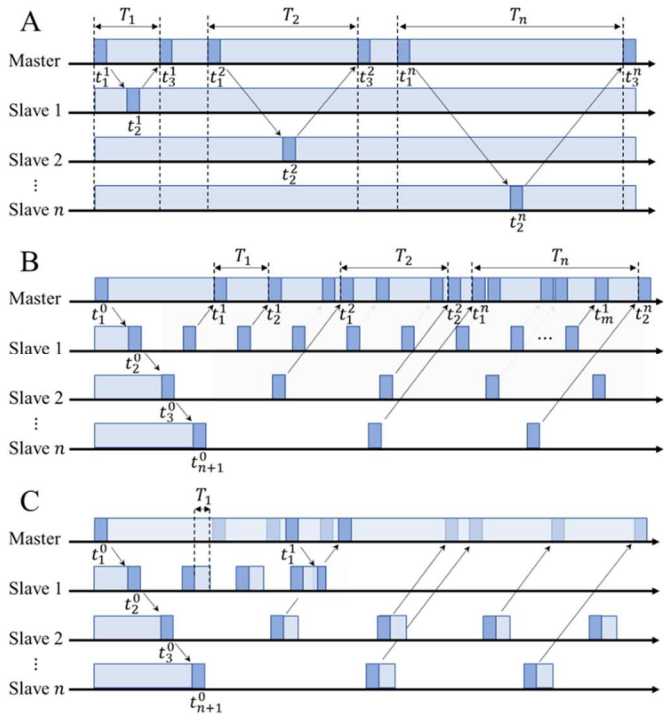

Fig. 4 Examples of the different pre-defined functionalities of the bidirectional tag: Polling-based transmission (A), Silent mode transmission (B), and Mixed mode transmission (C)

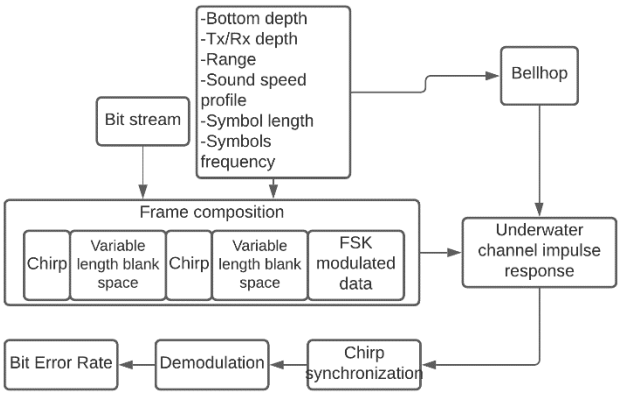

Fig. 5 Simulations block diagram. *The c*onfiguration parameters and a random bit-stream feed the modulation block and the bellhop block. *The r*esulting FSK frame is processed through underwater channel impulse response generated by Belhop. *Finally, t*he received signal is synchronized and demodulated and *the* bit error rate is computed.

On this simulation scenario, we can run a single simulation for a specific transmitter-receiver positions or a complete set of simulations for each transmitter-receiver position along the

whole scenario. In this way we can evaluate the modulation performance for different situations and bitrate/symbol duration. Fig. 8 shows simulation results for three different combinations of positions and symbol duration. Bottom depth is 500 m and transmitter is fixed on the bottom. The receiver depth switches between 350 m, 400 m and 450 m and the transmitter-receiver horizontal separation is fixed to 10 m. The symbol length varies from 0.798 ms to 10.374 ms and therefore, the estimated bit rate varies between 1250 bps to 96 bps. As we can see in the results, the largest symbol lengths provide a better performance against bit errors. Symbol lengths larger than 3 ms seems to perform greater in terms of bit error rate.

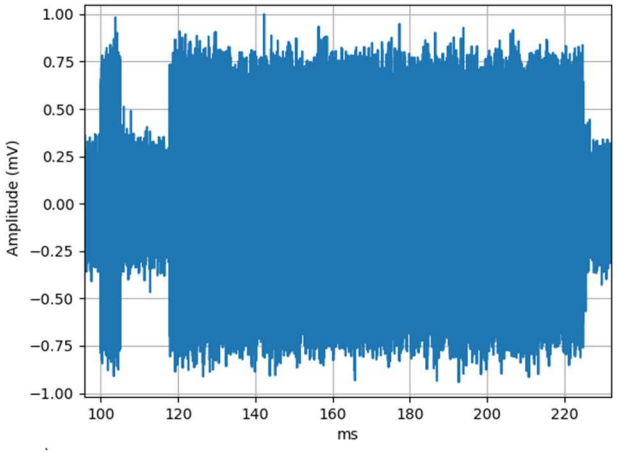

Fig. 6 Example of the received signal after it has been transmitted through the underwater acoustic channel generated by Bellhop. First signal is the 5 ms synchronization chirp followed by a blank space and the FSK frame

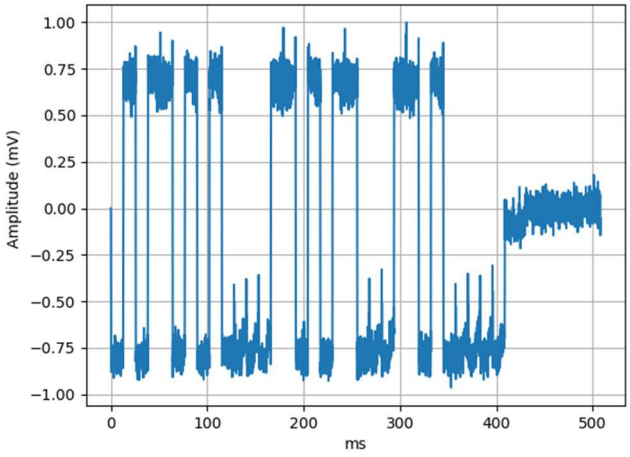

Fig. 7 Received signal after it has been processed through the complete receiver steps. The resulting synchronized baseband signal is sampled at symbol time to perform the decision procedure against a fixed threshold

With the objective of studying the system performance on the whole scenario, the same simulation approach can be extended to a wide range of transmitter-receiver positions. Fig. 9 and Fig. 10 show simulation results for a 1.596 ms symbol duration FSK frame. On the first case (Fig. 9) a receiver is fixed on the bottom and the transmitter is switched between all depth and range combinations. The second case (Fig. 10) is the opposite, the transmitter is fixed to the bottom and the receiver is switched across all depth and range combinations of the scenario. The spatial resolution is 1 m for range and 10 m for depth. In this way we can run a simulation for each combination of transmitter and receiver positions. For each simulation the bit error rate is computed, and an error map is generated with all the computed errors.

These simulation results are very helpful to obtain an initial estimation of the best spots where errors due to the multipath underwater channel are minimized. Positions around 400 meters depth and 20 – 200 meters range seems to be the best spots to avoid or minimize errors due to multipath channel effects.

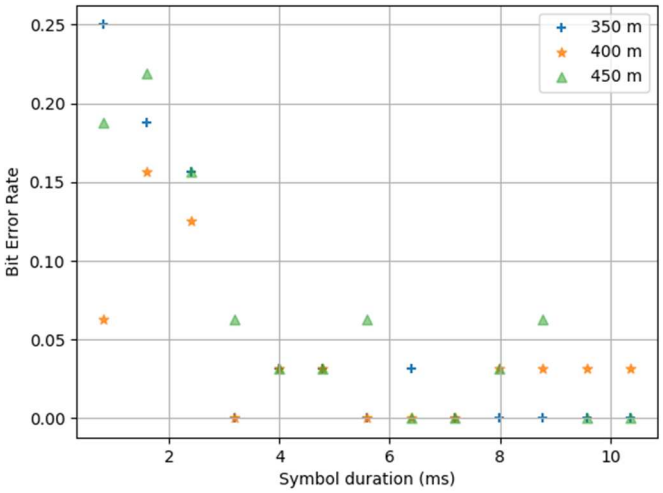

Fig. 8 Bit Error Rate vs symbol length simulation results for 3 specific scenarios. Ocean depth is 500 m, and the transmitter is fixed to the bottom. The range between the transmitter and the receiver is fixed to 10 m and receiver depth switches between 350 m, 400 m and 500 m.

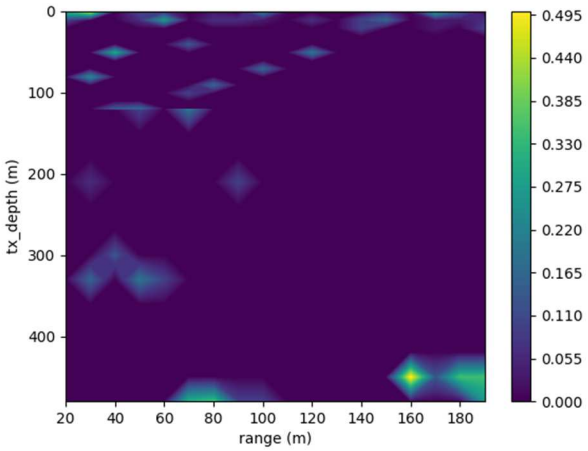

Fig. 9 Bit error rate map for different combinations of receiver-transmitter relative position with the receiver fixed to bottom and variable transmitter depth and separation from receiver

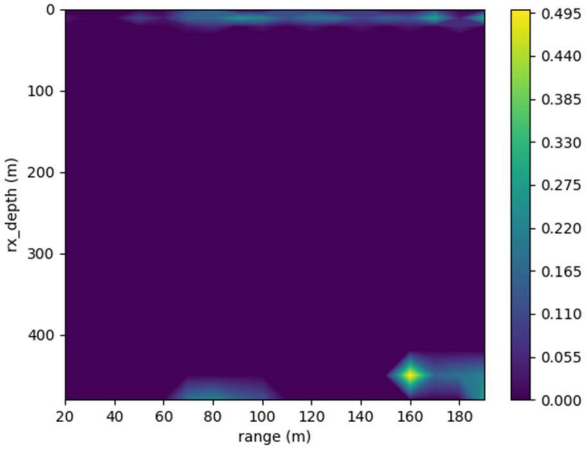

Fig. 10 Bit error rate map for different combinations of receiver-transmitter relative position with the transmitter fixed to bottom, variable receiver depth and separation from transmitter

IV. CONCLUSIONS

This work discusses the design of the communications of a new bidirectional acoustic tag. Due to its ease of implementation and low microcontroller resources demand, an FSK modulation scheme, both modulator and demodulator, has been implemented on the main unit of the tag. Underwater acoustic channel simulations lead to a first estimation of the best spots where underwater multipath effects are minimized, which are positions around 400 meters depth and transmitter-receiver horizontal distances between 20 and 200 meters. Symbol lengths between 3 ms to 10.374 ms presents the best performance against bit error rate. Three different predefined functionalities for the B-tag have been presented that implies different power consumption approaches, which are critical for these devices. We think that the different functionality modes implemented allows the B-tag to work on different scenarios such as marine animal tracking with autonomous underwater vehicles and range-based methods and the deployment of the tag as a part of a larger underwater sensors network [20]. Next step should be running the first field tests to validate simulation results.

ACKNOWLEDGMENT

This work has been led and carried out by members of the Tecnoterra associated unit of the Scientific Research Council through the *Universitat Politècnica de Catalunya*, the Jaume Almera Earth Sciences Institute and the Marine Science Institute (ICM-CSIC).

REFERENCES

[1] G. C. Hays et al., “Translating Marine Animal Tracking Data into Conservation Policy and Management,” Trends in Ecology and Evolution. 2019, vol. 34, pp. 459-473, May 2019.

[2] M. Stojanovic and P.-P. J. Beaujean, “Acoustic Communication,” Springer Handbook of Ocean Engineering, M. R. Dhanak and N. I. Xiros, Eds. Cham: Springer International Publishing, 2016, pp. 359–386.

[3] A. Song, M. Stojanovic, and M. Chitre, “Editorial Underwater Acoustic Communications: Where We Stand and What Is Next?,” IEEE Journal of Oceanic Engineering, vol. 44, no. 1. pp. 1–6, 2019.

[4] M. Chitre, R. Bhatnagar, M. Ignatius, and S. Suman, “Baseband signal processing with UnetStack,” 2014 Underwater Communications and Networking, UComms, Italy, pp. 1-4, September 2014.

[5] J. Alves, J. Potter, P. Guerrini, G. Zappa, and K. Lepage, “The LOON in 2014: Test bed description,” 2014 Underwater Communications and Networking, UComms, Italy, pp. 1-4,September 2014.

[6] H. S. Dol, P. Casari, T. Van Der Zwan, and R. Otnes, “Software-Defined Underwater Acoustic Modems: Historical Review and the NILUS Approach,” IEEE J. Ocean. Eng., vol, 42, pp, 722-737, July 2017.

[7] M. Stojanovic and L. Freitag, “Recent Trends in Underwater Acoustic Communications,” Mar. Technol. Soc., vol. 47, no. 5, pp. 45–50, September 2013.

[8] D. Kari, I. Marivani, F. Khan, M. O. Sayin, and S. S. Kozat, “Robust adaptive algorithms for underwater acoustic channel estimation and their performance analysis,” Digital Signal Processing, vol. 68, pp. 57-68, September 2017.

[9] M. Stojanovic, J. G. Proakis, and J. A. Catipovic, “Phase-Coherent Digital Communications for Underwater Acoustic Channels,” IEEE J. Ocean. Eng., 1994.

[10] O. Pallares, P. J. Bouvet, and J. Del Rio, “TS-MUWSN: Time Synchronization for Mobile Underwater Sensor Networks,” IEEE J. Oceanic Engineering, vol. 41, no. 4, October 2016.

[11] M. Stojanovic, “OFDM for underwater acoustic communications: adaptive synchronization and sparse channel estimation,” IEEE International Conference on Acoustics, Speech and Signal Processing - Proceedings, pp. 5288-5291, USA 2008.

[12] G. Qiao, Z. Babar, L. Ma, S. Liu, and J. Wu, “MIMO-OFDM underwater acoustic communication systems—A review,” Physical Communication, vol. 23, pp. 56-64. June 2017.

[13] S. Zhou and Z. Wang, OFDM for Underwater Acoustic Communications. Wiley, June 2014.

[14] J. C. Peterson and M. B. Porter, “Ray/beam tracing for modeling the effects of ocean and platform dynamics,” IEEE Journal of Oceanic Engineering, vol. 38, no. 4, pp. 655-665, October 2013.

[15] O. Carmago, “General description of the BELLHOP ray tracing program.”, Signal Processing Laboratory, Universidade do Algarve, June 2008.

[16] P. Qarabaqi and M. Stojanovic, “Statistical characterization and computationally efficient modeling of a class of underwater acoustic communication channels,” IEEE Journal Oceanic Engineering, vol. 38, no. 4, pp. 701-717, October 2013.

[17] I. Masmitja, D. Corregidor, J.M. López, E. Martínez, J. Navarro, S. Gomariz, "Miniaturised bidirectional acoustic tag to enhance marine animal tracking studies," IEEE International Instrumentation and Measurement Technology Conference, in press.

[18] A. K. Morozov and J. C. Preisig, “Underwater acoustic communications with multi-carrier modulation,” pp. 1-6, OCEANS 2006, Boston USA 2006.

[19] D. Miorandi and S. Vitturi, “Analysis of master-slave protocols for real-time industrial communications over IEEE802.11 WLANs,” 2nd IEEE International Conference on Industrial Informatics, pp. 143-148, Berlin Germany 2004.

[20] I. Masmitja et al., "Mobile robotic platforms for the acoustic tracking of deep-sea demersal fishery resources," Science Robotics, vol. 5, no. 48, November 2020.